Supporting Information

A Microelectrochemical Flow Cell for Studying Electrocatalytic Reactions on Oxide-Coated Electrodes

Morgan J. Anderson, Nevena Ostojic, Richard M. Crooks

Table of Contents

Chemicals and materials. Unless otherwise stated, all chemicals were used as received. These include: 1,1′-ferrocenedimethanol ($Fc(MeOH)_2$, 98%, Acros Organics, NY), $HClO_4$ (+70%, ultrapure grade, J.T. Baker). The following chemicals were purchased from Sigma Aldrich: $CuSO_4$ (98%), $NaBH_4$ (99.99%), K_2PtCl_4 (99.99%). Sixth-generation, hydoxyl-terminated, poly(amidoamine) (G6-OH) dendrimers were purchased as a 10-25% methanol solution from Dendritech, Inc. (Midland, MI). Prior to use, methanol was removed under vacuum.

Trimethylaluminum (TMA) for ALD was obtained in sealed stainless steel canister from Sigma-Aldrich. High-purity (99.9999%) N_2 for ALD, high-purity (99.9999%) O_2 for ALD and UV/O_3 system, and a mixed 5% H_2/95% N_2 gas for pyrolysis of photoresists were purchased from Praxair (Austin, TX).

Quartz slides were purchased from Technical Glass Products (Painesville Twp, OH). AZ 1518 photoresist and AZ 400K developer (pre-diluted 1:4) were purchased from Integrated Micro Materials (Argyle, TX). Acrylic sheets and silicone gaskets were purchased from McMaster Carr (Atlanta, GA). NanoPorts and fluidic connections were purchased from Idex Health and Science (Oak Harbor, WA).

Deionized (DI) water having a resistivity of 18.2 MΩ-cm (Milli-Q Gradient, Millipore, Billerica, MA) was used for the preparation of all aqueous solutions.

Fabrication of Pt collector electrodes. Pt collector electrodes were fabricated by physical vapor deposition. Electrodes consisted of a 20 nm Ti adhesion layer and 100 nm Pt deposited onto 2.5 cm x 7.5 cm unpatterned glass slides. Following deposition, the slides were cut into 2.5 cm x 2.5 cm pieces and rinsed with ethanol prior to use.

Fabrication of pyrolyzed photoresist film (PPF) electrodes. The PPF electrodes[1-5] were fabricated following a previously published procedure.[6] Briefly, quartz slides were cleaned sequentially in acetone, ethanol, and DI water for 10 min each. The slides were further rinsed under running DI water for 1 min and then heated at 200 °C for 15 min. After cooling to room

temperature (24 ± 1 °C), positive-tone AZ 1518 photoresist was spin-coated onto the slides for 10 s at 500 rpm, 45 s at 3500 rpm, and for 5 s at 500 rpm. Finally, the slides were soft baked for 1 min at 100 °C and left to cool to room temperature. The spin coating and soft baking processes were then repeated a second time.

The photoresist-coated quartz slides were patterned by exposure to UV light through a photomask. Next, AZ 400 K developer, diluted to 25% (v/v) with DI water, was used to develop the exposed photoresist. Finally, the photoresist was pyrolyzed in a quartz tube furnace under a constant flow (100 sccm) of forming gas (5% H_2/95% N_2). The furnace temperature was increased from 25 °C to 1000 °C at 5 °C/min, held at 1000 °C for 1 h, and then cooled to 25 °C. The resulting PPF slide was then diced into individual electrodes using a diamond-tipped pen. The individual PPF electrodes were gently rinsed with ethanol and dried under flowing N_2.

Prior to ALD, the PPFs were activated with UV/O_3 using a commercial UV/O_3 system (PSD-UV4 with OES1000D, Novascan Technologies, Ames, IA). Individual PPFs were placed in the center of the chamber ~2 cm from the UV lamp. The vacuum was turned on, and after 5 min an external supply of O_2 was introduced into the chamber at 259 mmHg for 5 min. The O_2 flow was then stopped and the UV lamp was turned on for 10 min. After the UV/O_3 treatment, PPFs were loaded into the ALD chamber within 2 min.

X-ray photoelectron spectroscopy (XPS). XPS samples were prepared by immobilizing Pt DENs atop Al_2O_3-modified PPF electrodes as previously described. XPS was carried out using a Kratos Axis Ultra spectrometer (Chestnut Ridge, NY) having an Al K_α source. Samples were grounded using metal holders. Careful placement of the PPF/Al_2O_3/G6-OH(Pt_{55}) electrode made it possible to characterize the same location before and after UV/O_3 treatment. This was important because the G6-OH(Pt_{55}) aliquot did not dry uniformly on the Al_2O_3 support.

XPS spectra were collected using a 0.10 eV step size and a band pass energy of 20 eV. Binding energies (BEs) were calibrated against the C 1s carbonyl peak of G6–OH dendrimer (288.5 eV).[7,8] CasaXPS (version 2.3.15, Casa Software, Teignmouth, UK) was used for peak fitting and analysis. A mixed Gaussian/Lorentzian model was used for symmetric line-shapes, while an asymmetric Lorentzian model was applied for asymmetric line shapes.

Transmission electron microscopy (TEM). TEM images were obtained using a JEOL-2010F transmission electron microscope having a point-to-point resolution of 0.19 nm. Samples were prepared by pipetting 2.0 μL of the G6–OH(Pt_{55}) solution onto a continuous carbon-over-Cu TEM grid (Electron Microscopy Sciences, Hatfield, PA) and then drying in air overnight.

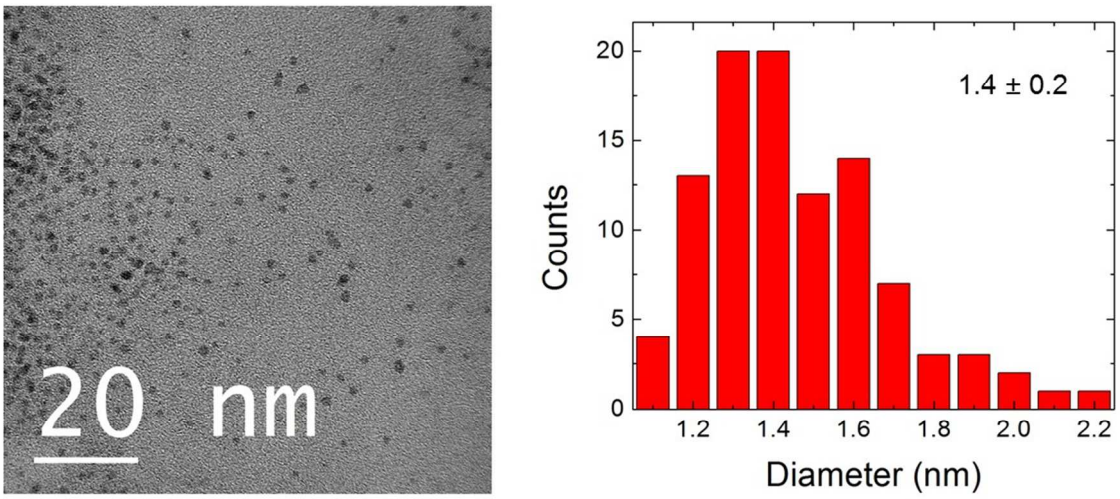

Figure S1. (Left) Transmission electron micrograph and (right) size-distribution histogram for the G6-OH(Pt_{55}) DENs used in this work.

Details of flow cell fabrication. The flow cell was constructed from layers of 500 µm-thick silicone and 6.3 mm-thick acrylic sheets. The silicone and acrylic pieces were cut using a commercial CO_2 laser cutter (Epilog Zing 16, 30W, Golden, CO). Silicone sheets were cut using 10% power, 100% speed, and 5000 Hz frequency. Acrylic sheets were cut using 100% power, 5% speed, and 5000 Hz frequency.

The individual pieces of the flow cell were prepared as follows, starting from the bottom of Scheme 2a in the main text. The laser was rastered (3 passes at 40% speed and 80% power) across the acrylic base layer to create two 2.5 cm x 2.5 cm recessions to accommodate the GE and CE (Figure S2a). The electrodes were placed in the base acrylic layer and affixed with Cu tape (Figures S2b and S2c). The lower silicone gasket was cut to create two separate channel segments and seal the edges to prevent leaking where the electrodes and the acrylic base layer meet (Figure S2d). This silicone layer resulted in a gap of between 10.1 and 11.5 mm between the two electrodes, constrained the width of the channel to 500 µm, and limited the CE length exposed to the flowing solution to 7.6 mm. The acrylic bridge layer was fabricated by rastering the laser (2 passes at 80% speed and 100% power) across the surface to create a lip around the channel. This layer was further etched (4 passes at 80% speed and 100% power) to create a fluidic pathway for solution to flow between the two silicone channel sections (Figure S2e). Holes were cut through this acrylic layer for solution to flow to the channel layer.

The upper silicone gasket was cut to size, and then holes were added for fluid flow (Figure S2f). This sheet creates a seal between the bridge acrylic layer and the NanoPorts. The top acrylic layer was etched to accommodate the lip of the NanoPorts, hold them in place, and create a seal between the NanoPort assembly and the upper silicone gasket when the cell is secured (Figure S2g).

The flow cell was assembled as illustrated in Scheme 2a (main text) and secured with nuts (Figure S2h). The nuts were

tightened in a cross pattern to evenly distribute pressure across the electrodes. One of the NanoPorts was connected to a syringe pump (Pico Pump Elite, Harvard Apparatus, Holliston, MA) outfitted with a 10 mL gas-tight syringe (Model 1010, Hamilton, Franklin, MA) and PEEK tubing. The other NanoPort was connected to an outlet reservoir where the reference and counter electrodes were placed. Figure S3 is a photograph of the assembled flow cell.

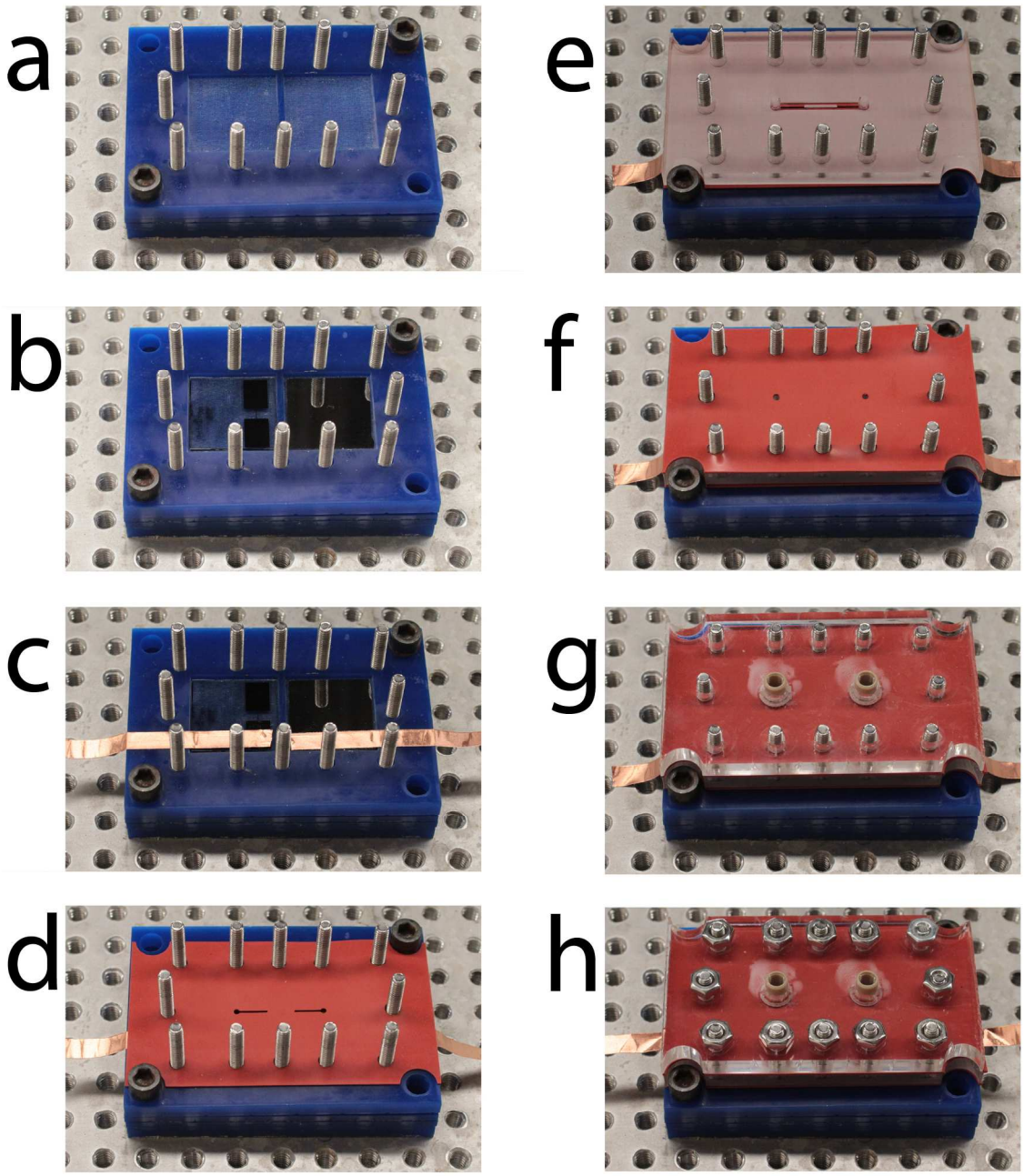

Figure S2. Photographs showing the step by step assembly of the flow cell used in this work.

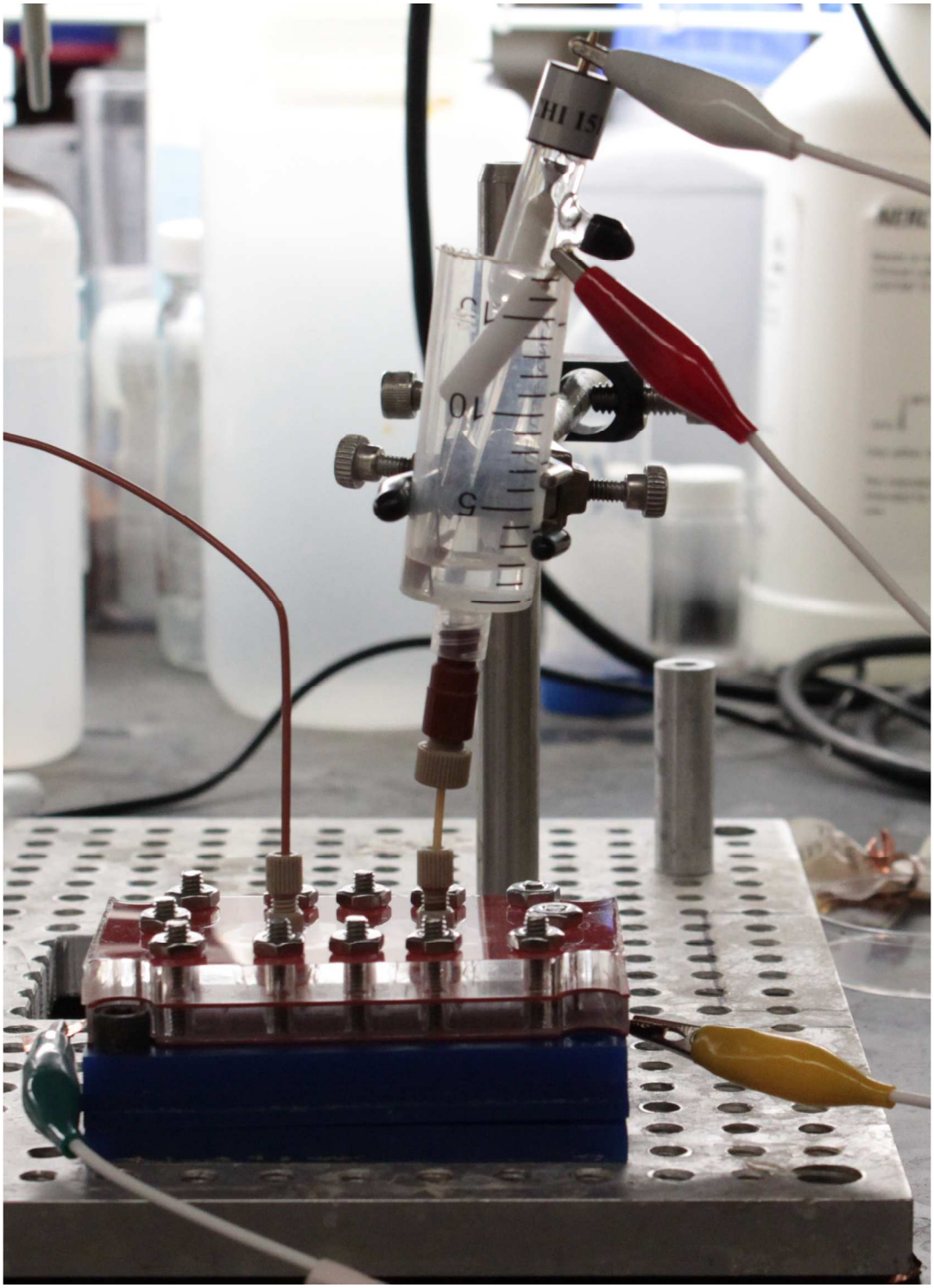

Figure S3. A photograph of the assembled flow cell.

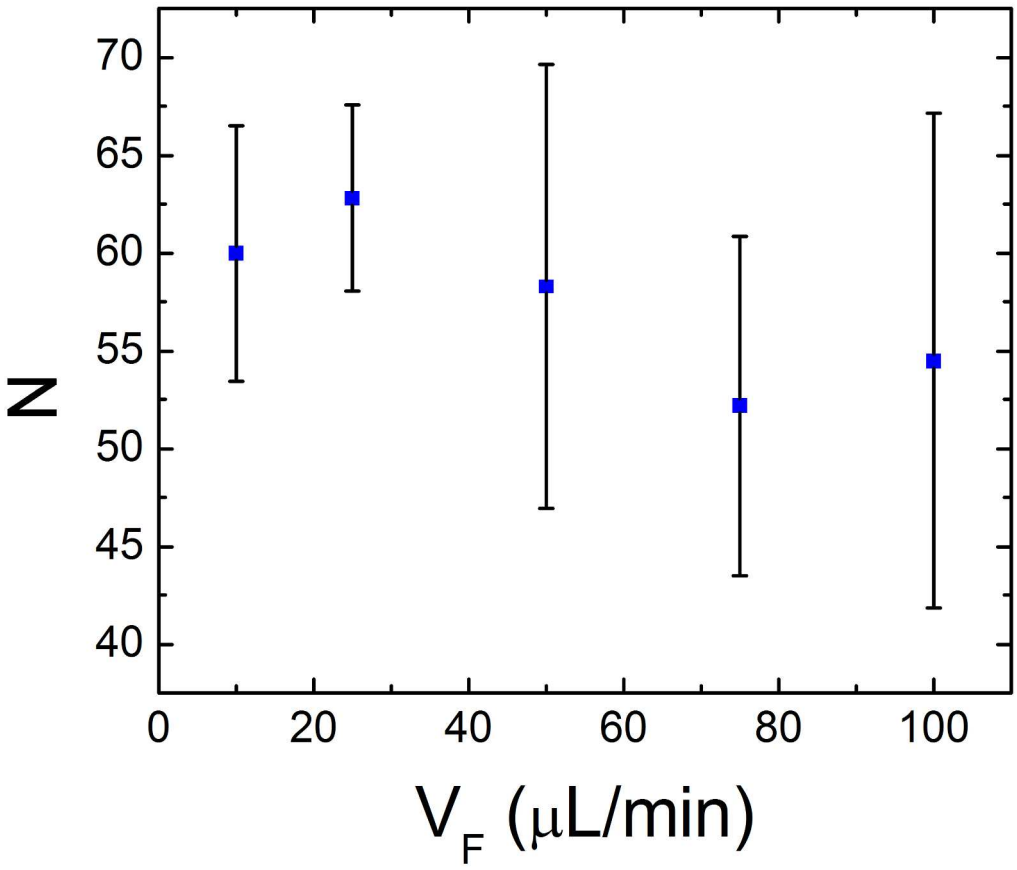

Figure S4. Measured collection efficiencies (N) as a function of volumetric flow rate (V_F). The GE was stepped from −0.50 V to 0.20 V while holding the CE at −0.50 V in a flowing solution containing 0.10 M KNO_3 and 1.0 mM $Fc(MeOH)_2$. The resulting values of i_L^{GE} and i_L^{CE} were used to calculate N based on eq 1 in the main text. The error bars represent the standard deviation from the mean for four independent measurements (using a different electrode for each set of measurements) at each flow rate.

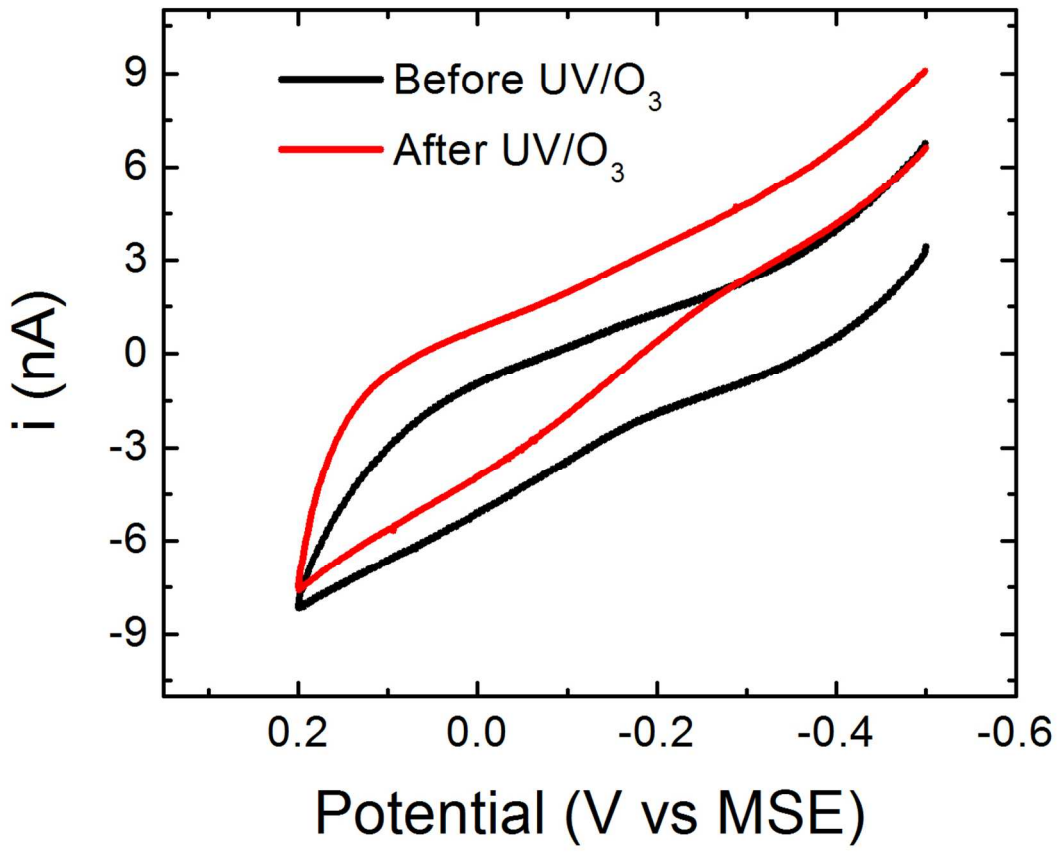

Figure S5. Cyclic voltammograms (CVs) of a PPF/Al_2O_3 electrode (a) before and (b) after UV/O_3 treatment. The electrode was scanned once from −0.50 V to 0.20 V and back to −0.50 V (scan rate = 0.060 V/s) in a flowing (50 µL/min) aqueous solution containing 1.0 mM $Fc(MeOH)_2$ and 0.10 M KNO_3.

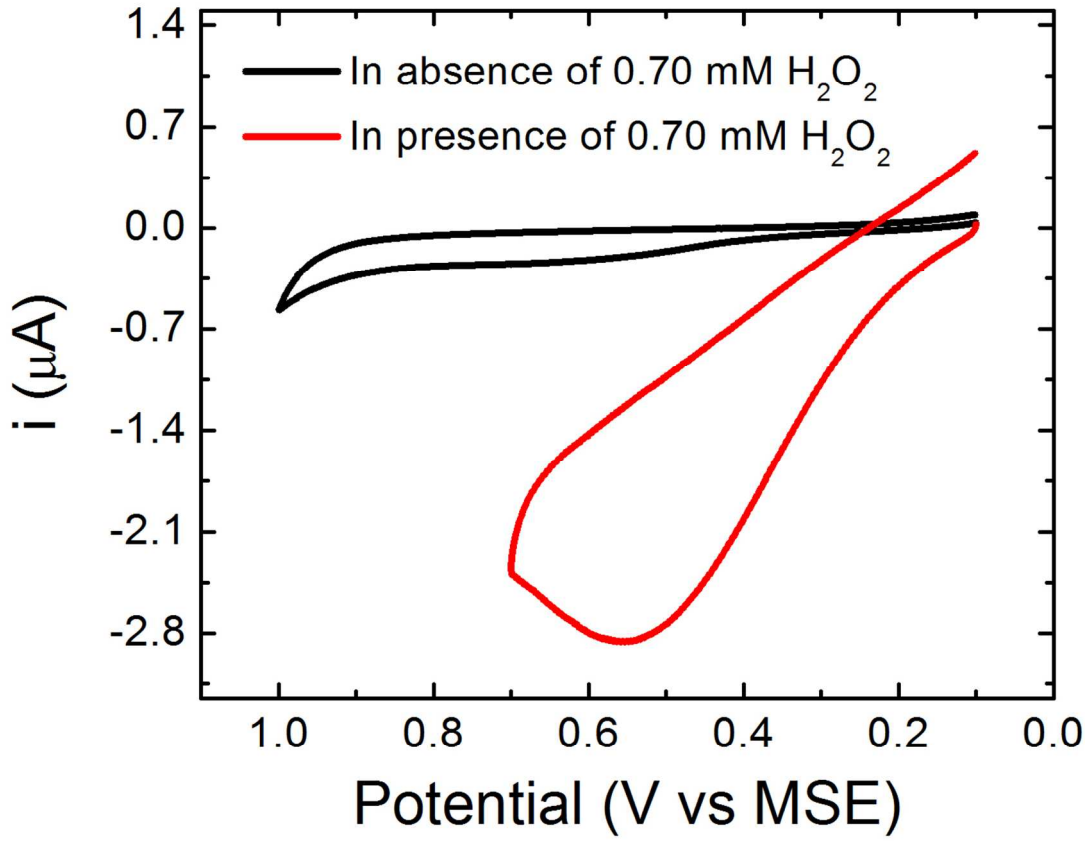

Figure S6. Diffusion-controlled oxidation of H_2O_2 at a platinized PPF electrode. CVs of a platinized PPF GE in an aqueous 0.10 M $HClO_4$ solution in absence and presence of 0.70 mM H_2O_2. The flow rate used was 5.0 μL/min and the scan rate was 0.060 V/s. The results show that a potential of O.70 V is sufficient to oxidize H_2O_2 to O_2 at the mass transfer-limited rate. Accordingly, the CE was set to this potential for the generator-collector experiments described in the main text.

References

(1) Kim, J.; Song, X.; Kinoshita, K.; Madou, M.; White, B. *J. Electrochem. Soc.* **1998**, *145*, 2314–2319.

(2) Ranganathan, S.; McCreery, R. L. *Anal. Chem.* **2001**, *73*, 893–900.

(3) Kostecki, R.; Schnyder, B.; Alliata, D.; Song, X.; Kinoshita, K.; Kötz, R. *Thin Solid Films* **2001**, *396*, 36–43.

(4) Dumitrescu, I.; Crooks, R. M. *Proc. Natl. Acad. Sci., USA* **2012**, *109*, 11493–11497.

(5) Dumitrescu, I.; Yancey, D. F.; Crooks, R. M. *Lab Chip* **2012**, *12*, 986.

(6) Ostojic, N.; Crooks, R. M. *Langmuir* **2016**, *32*, 9727–9735

(7) NIST X-Ray Photoelectron Spectroscopy Database, Version 4.1, National Institute of Standards and Technology: Gaithersburg, MD http://srdata.nist.gov/xps/.

(8) Ozturk, O.; Black, T. J.; Perrine, K.; Pizzolato, K.; Williams, C. T.; Parsons, F. W.; Ratliff, J. S.; Gao, J.; Murphy, C. J.; Xie, H.; *et al. Langmuir* **2005**, *21*, 3998–4006.